PCCP

Accepted Manuscript

ROYAL SOCIETY OF CHEMISTRY

www.rsc.org/pccp

4-Hydroxy-1-naphthaldehydes: proton transfer or deprotonation.

Y. Manolova, V. Kurteva and L. Antonov*

Institute of Organic Chemistry with Centre of Phytochemistry, Bulgarian Academy of Sciences, Acad. G.Bonchev str., bldg. 9, Sofia 1113, Bulgaria

H. Marciniak and S. Lochbrunner

Institut für Physik, Universität Rostock, Universitätsplatz 3, 18051 Rostock, Germany

A. Crochet and K.M. Fromm

Department of Chemistry, University of Fribourg, Chemin du Musée 9, 1700 Fribourg, Switzerland

F.S. Kamounah and P.E. Hansen

Department of Science, Systems and Models, Roskilde University, Universitetsvej 1, P.O.Box 260, DK-4000 Roskilde, Denmark

Abstract:

A series of naphthaldehydes, including a Mannich base, have been investigated by UV-Vis spectroscopy, NMR and theoretical methods to explore their potential tautomerism. In the case of 4-Hydroxy-1-naphthaldehyde a process of concentration dependent deprotonation has been detected in methanol and acetonitrile. For 4-Hydroxy-3-(piperidin-1-ylmethyl)-1-naphthaldehyde (a Mannich base) an intramolecular proton transfer involving the OH group and the nitrogen of the piperidine nitrogen exists. In acetonitrile the equilibrium is predominantly at the OH-form, whereas in methanol the proton transferred tautomer is the preferred form. In chloroform, methylene chloride and toluene the OH form is completely dominant. Both 4-Hydroxy-1-naphthaldehyde and 4-Methoxy-1-naphthaldehyde (fixed enol form) show a dimerization in the investigated solvents and the crystallographic data, obtained for the latter, confirms the existence of a cyclic dimer.

Keywords: tautomerism, proton transfer, UV-spectroscopy, NMR, dimerization

* Corresponding author: http://www.orgchm.bas.bg/~i2mp

Introduction:

The concept of molecular electronics [1,2,3], being based on the use of single molecules as building elements (wires, switches, rectifiers, etc.) and their further suitable assembly into working devices, catalyzes intensive investigations in order to find such molecular level "hardware". The main emphasis is given to organic and hybrid systems, because a wide range of molecular propensities can be combined with the versatility of synthetic chemistry to alter and optimize molecular structure in the direction of desired properties.

Virtually, every single molecule changes its behavior when acted upon by external stimuli, but its use as a molecular switch is possible only if these changes are reproducible, reversible and can be controlled and monitored [4]. Among the variety of types [5] of switching systems, several systems based on tautomeric proton exchange have recently been reported [6,7,8]. It is not surprising that the tautomerism attracts attention in this field - the main requirement in the design of molecular switches is to provide fast and clean interconversion between structurally different molecular (on- and off-) states and the tautomerism is an excellent possibility, because the change in the tautomeric state is accomplished by a fast proton transfer reaction between two or more structures, each of them with clearly defined and different molecular properties. The main problem [9] is to provide conditions for a controlled shift of the tautomeric equilibrium in a way that the on- and off-states correspond to the individual tautomers.

The conceptual idea of a keto-enol tautomeric switch, developed recently by us, is presented in Figure 1 [7,10,11]. On one side, the enol-like off-state is achieved by engagement of the tautomeric proton in an intramolecular hydrogen bond with a macrocyclic antenna, connected to the tautomeric unit by a spacer. On the other side, the engagement of the same antenna by external stimuli (like the addition of an acid [7] or metal ions [10]) causes a change in the tautomeric state, switching to the keto-like on-state.

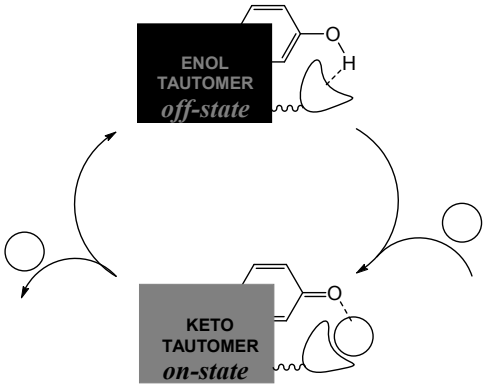

Figure 1. Control of the switching in a keto-enol tautomeric system.

The real switching requests a moderate energy gap between the individual (i.e. without attached antenna) tautomeric building blocks, because the stabilizing effect of the neutral antenna on the enol form and the stabilizing effect of the protonated antenna on the keto form vary depending on the tautomeric compound. For instance, the switching in solution with a piperidine antenna is possible in azonaphthols and related Schiff bases, where the relative energy between individual tautomers is ~ 1.5 kcal/mol and ~ 4 kcal/mol (the enol form more stable) resp., but impossible in azophenols where the energy gap is more than 10 kcal/mol [7,11]. In addition the size of these systems does not allow detailed theoretical studies applying sophisticated DFT functionals with large basis sets.

For this reason, we concentrate our efforts in the current communication on the possibilities of switching in 4-Hydroxy-1-naphthaldehyde (**1**) and its analogue with an attached piperidine antenna (**2**). Compound **1** is potentially tautomeric, but from its structure it is clear that switching from the enol to the keto form could lead to a destabilization due to the loss of aromaticity of the naphthalene ring. Therefore it represents a suitable example to model processes of switching in systems with a large energy gap between individual tautomers. To the best of our knowledge no detailed theoretical and experimental investigation of the spectral behavior of these two compounds has been carried out up to now, taking into account that the general template for synthesis of compound **2** was recently reported for the first time [12]. In addition, the interpretation of the results is supported by the study of compounds **3** and **4**, which model different aspects of the behavior of **1** in solution.

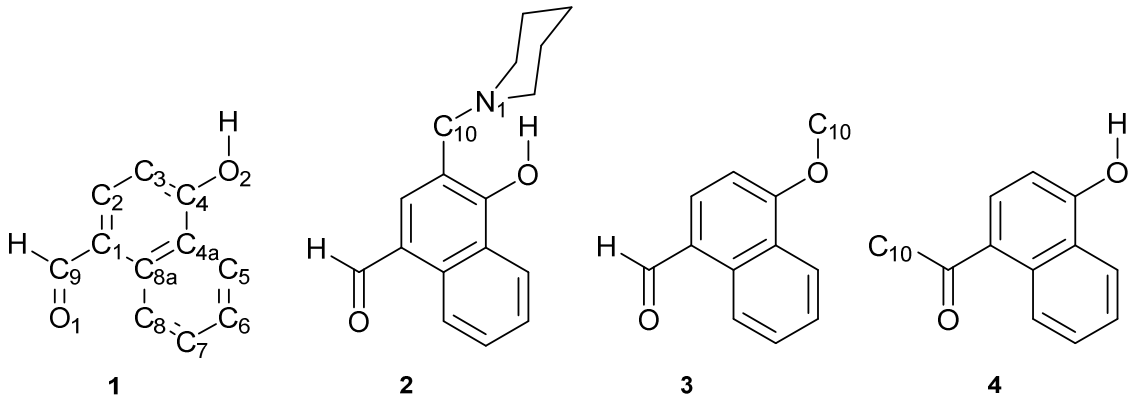

Scheme 1. Compounds under investigation with numbering of the heavy atoms.

Experimental part

General:

All reagents were purchased from Merck, Aldrich and Fluka and were used without any further purification. Fluka silica gel/TLC-cards 60778 with fluorescent indicator 254 nm were

used for TLC chromatography. The melting points were determined in capillary tubes on a SRS MPA100 OptiMelt (Sunnyvale, CA, USA) automated melting point system. The NMR spectra were recorded on a Bruker Avance II+ 600 spectrometer at 25°C or at a Varian Mercury 300 system; the chemical shifts were quoted in ppm in δ-values against tetramethylsilane (TMS) as an internal standard and the coupling constants were calculated in Hz. The assignment of the signals was confirmed by applying 2D techniques. The spectra were recorded as $3x10^{-2}$ M solutions in order to avoid transmolecular interactions in the NOESY experiments. The spectra were processed with the Topspin 2.1 program.

Compound **1** was purchased from Aldrich (No. 131067).

Compound **2** (***4-Hydroxy-3-(piperidin-1-ylmethyl)-1-naphthaldehyde*** [12]) was synthesized according to the following procedure: To a solution of piperidine (2.2 mmol) in benzene (15 ml) paraformaldehyde (2.2 mmol), *p*-toluenesulfonic acid (15 mg), and then 4-hydroxy-1-naphthaldehyde (2 mmol) were added and the mixture was refluxed with stirring for 3 h. The products were partitioned between benzene and water. The organic phase was dried over Na_2SO_4, evaporated to dryness, and purified by HPFC or flash chromatography on silica gel by using a mobile phase with a gradient of polarity from CH_2Cl_2 to acetone-CH_2Cl_2 1:9 to obtain pure **2**: 85 % yield; R_f 0.34 (acetone-CH_2Cl_2 1:9); light yellowish solid, m. p. 106.7-106.9°C; ^{1}H NMR ($CDCl_3$, 600 MHz) 1.382 (bs, 2H, C*H*$_2$-4 piperidine), 1.739 (bs, 4H, C*H*$_2$-3 and C*H*$_2$-5 piperidine), 2.248 (bs, 2H, ½ of C*H*$_2$-2 and C*H*$_2$-6 piperidine), 3.100 (bs, 2H, ½ of C*H*$_2$-2 and C*H*$_2$-6 piperidine), 3.930 (s, 2H, Ar-C*H*$_2$-N), 7.565 (ddd, 1H, J 1.2, 6.8, 8.2, C*H*-6 Ar), 7.607 (s, 1H, C*H*-2 Ar), 7.681 (ddd, 1H, J 1.4, 6.8, 8.3, C*H*-7 Ar), 8.350 (ddd, 1H, J 0.7,1.4, 8.4, C*H*-5 Ar), 9.257 (ddd, 1H, J 0.8, 1.0, 8.5, C*H*-8 Ar), 10.167 (s, 1H, C*H*=O), 10.639 (bs, 1H, O*H*); ^{13}C NMR 23.73 (*C*H$_2$-4 piperidine), 25.64 (*C*H$_2$-3 and *C*H$_2$-5 piperidine), 53.77 (*C*H$_2$-2 and *C*H$_2$-6 piperidine), 61.66 (Ar-*C*H$_2$-N), 112.67 (*C*$_{quat}$-3), 122.47 (*C*$_{quat}$-1), 122.69 (*C*H-5 Ar), 124.49 (*C*H-8 Ar), 125.18 (*C*$_{quat}$-4a), 125.82 (*C*H-6 Ar), 129.32 (*C*H-7 Ar), 131.92 (*C*$_{quat}$-8a), 138.95 (*C*H-2 Ar), 162.20 (*C*$_{quat}$-4), 191.56 (*C*H=O); COSY cross peaks 7.565/7.607, 7.565/8.350, 7.607/9.257; NOESY cross peaks 1.382/1.739, 1.739/2.248 (weak), 1.739/3.100 (weak), 2.248/3.100, 2.248/3.930 (weak), 3.100/3.930 (weak), 3.930/7.607, 7.565/7.681, 7.565/8.350, 7.607/10.167, 7.681/9.257, 9.257/10.167; HSQC cross peaks 1.382/23.73, 1.739/25.64, 2.248/53.77, 3.100/53.77, 3.930/61.66, 7.565/125.82, 7.607/138.95, 7.681/129.32, 8.350/122.69, 9.257/124.49, 10.167/191.56; HMBC cross peaks 1.739/23.73 (weak), 3.930/53.77, 3.930/112.67, 3.930/138.95, 3.930/162.20, 7.565/124.49, 7.565/125.18, 7.607/61.66, 7.607/131.92, 7.607/162.20, 7.607/191.56, 7.681/122.69, 7.681/131.92, 8.350/129.32, 8.350/131.92, 8.350/162.20, 9.257/122.47, 9.257/125.18, 9.257/162.20 (weak), 10.167/122.47, 10.167/131.92, 10.167/138.95.

Compound **3** (***4-Methoxy-1-naphthaldehyde*** [13]) was synthesized as follows: A mixture of 1-hydroxy-4-naphthaldehyde (1 mmol), NaOH (2 mmol) and CH_3I (10 mmol) in dry THF (20 ml) was stirred at room temperature for 6 h. The solvent was removed in *vacuo* and the products were purified by HPFC on silica gel using a mobile phase with a gradient of polarity

from DCM to 1 % acetone/DCM to give pure **3**: 98 % yield; R_f 0.62 (1 % acetone/DCM); m. p. 34.2-34.6°C (lit. [13] 34°C); ^{1}H NMR ($CDCl_3$, 600 MHz) 4.077 (s, 3H, OC*H*$_3$), 6.893 (d, 1H, J 8.1, C*H*-3), 7.559 (ddd, 1H, J 1.3, 6.9, 8.3, C*H*-6), 7.687 (ddd, 1H, J 1.4, 6.9, 8.4, C*H*-7), 7.896 (d, 1H, J 8.1, C*H*-2), 8.318 (ddd, 1H, J 0.7,1.3, 8.4, C*H*-5), 9.297 (ddd, 1H, J 0.7, 1.1, 8.6, C*H*-8), 10.191 (s, 1H, C*H*=O); ^{13}C NMR 55.98 (O*C*H$_3$), 102.92 (*C*H-3), 122.38 (*C*H-5 Ar), 124.87 (*C*H-8), 125.02 (C_{quat}-1), 125.53 (C_{quat}-4a), 126.40 (*C*H-6), 129.53 (*C*H-7), 131.90 (C_{quat}-8a), 139.64 (*C*H-2), 160.85 (C_{quat}-4), 192.27 (*C*H=O).

Compound **4** (***1-Acetyl-4-hydroxynaphthalene***): Acetyl chloride (2.4 g, 30.8 mmol) is dissolved in anhydrous nitromethane (10.0 ml) and, while stirring, added drop wise to a mixture of 1-naphthol (4.0 g, 27.8 mmol) and zinc chloride (4.0 g, 29.3 mmol) in anhydrous nitromethane (40.0 ml) at 0 ^{0}C (ice-bath) with vigorous stirring under anhydrous condition. After complete addition, the mixture is stirred at 0 ^{0}C for 30 minutes, then the ice bath removed and the mixture left stirred at room temperature for 20 h. The reaction mixture is poured onto 300 g of ice and 12.0 ml of concentrated hydrochloric acid with continuous stirring for 30 minutes. Dichloromethane (100.0 ml) is added and the organic layer is separated, washed with water (3x100 ml), brine and finally dried over anhydrous sodium sulfate. Evaporation of solvent in *vacuo* affords light brown solid residue. The residue is purified by chromatography on silica gel eluting with dichloromethane/ethyl acetate (20:1) to afford creamy solid (1.79 g, 56% yield), m.p. 199-200 ^{0}C, *m/e* 186.2. ^{1}H NMR (CDCl3, 300 MHz) 2.72 (s, 3H, CH3), 6.28 (s, 1H, OH), 6.83 (d, J. /.8 Hz, 1H, *CH-3* Ar), 7.55 (m, J= 8.4 and 6.9 Hz,1H, *CH-6* Ar), 7.65 (m, J= 8.7 and 6.9 Hz,1H, *CH-7* Ar), 7.96 (d, J=8.7 Hz, 1H, *CH-2* Ar), 8.27 (dm, J= 8.7 Hz,1H, *CH-5* Ar), 9.04 (dt, J= 8.7 and 0.6 Hz, 1H, *CH-8*Ar). The chemical shifts are almost identical to those given in [14]. ^{13}C NMR ($CDCl_3$, 75 MHz), 29.57 (CH_3), 107.06 (C-3), 122.06 (C-1), 124.78 (C-4a), 126.07 (C-6), 126.64 (C-8), 127.82 (C-6), 129.20 (C-7), 131.96 (C-2), 132.98 (C-8a), 156.13 (C-4), 200.42 (C=O). However, the claimed compound to be used for comparison (15) turned out to be 2-acetyl-1-hydroxynaphthalene.

Spectral investigations:

The UV-Vis spectral measurements were performed on a JASCO V-570 UV-Vis-NIR spectrophotometer, equipped with a Huber MPC-K6 thermostat (precision 1°C), in spectral-grade solvents. The concentration effects were studied in acetonitrile and methanol, keeping the product of cell thickness (b) and total compound concentration (c°) constant by using cells with a thickness varying from 0.1 to 10 cm. Diluted solutions of 95-97% sulfuric acid (pure for analysis) were used for the protonation in acetonitrile and methanol. The deprotonation was performed by addition of NaOH (in methanol) or NH_4OH (in acetonitrile). The pH values were measured with Metrohm 654 pH meter.

Quantitative analysis of the processes of deprotonation and aggregation was performed by using a “fishing net” algorithm, for which the mathematical background and applications have been already described [16]. The results have been statistically verified according to [17].

X-ray measurements:

Single crystals of compound **3** were obtained from methanol at room temperature after crystallization for 9 days. The obtained compound crystallizes as colorless needles in the monoclinic space group $P2_1/n$ (No. 14). The structure was solved with the program Shelx2014 [18], and revealed formation of pairs of molecules via hydrogen bonding in the solid state (Figures 1 and 2). The electron density map (Figures S1-S3) clearly shows a disorder of aldehyde and acid functions. This is due to oxidation of the aldehyde by air into the corresponding acid. Indeed, the position of the carbonyl oxygen atom of the aldehyde superposes with the one from the acid function, while the H-atom of the aldehyde and the OH-group of the acid are also almost superimposed. The relative amounts of aldehyde versus acid have been best refined as 60:40 (see the Supplementary information). The hydrogen bonds between O1#1 (#1 -x+1,-y+1,-z+1) and O3 are 2.599(5) Å. Compared to the mean plane of the aromatic ring, the aldehyde/acid group is in the plane. The pairs of molecules arrange into chains along the *c*-axis direction (Figure S4) and further packing along the *b*-axis is shown in Figure S5.

The crystallographic data of **3** were deposited at the Cambridge Crystallographic Data Centre with deposition number CCDC 1043758. Copies of the data can be obtained, free of charge, on application to CCDC, 12 Union Road, Cambridge CB2 1EZ, UK; phone: +44 1223 762910; fax: +44 1223 336033; e-mail: deposit@ccdc.cam.ac.uk

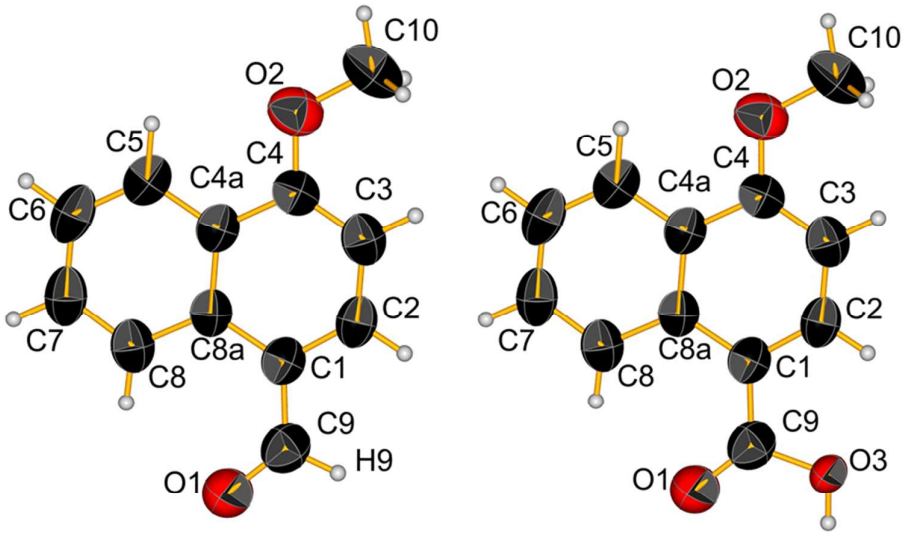

Figure 1. Ortep representation of the aldehyde form (left) and the acid (right), ellipsoids are drawn with 50% of probability.

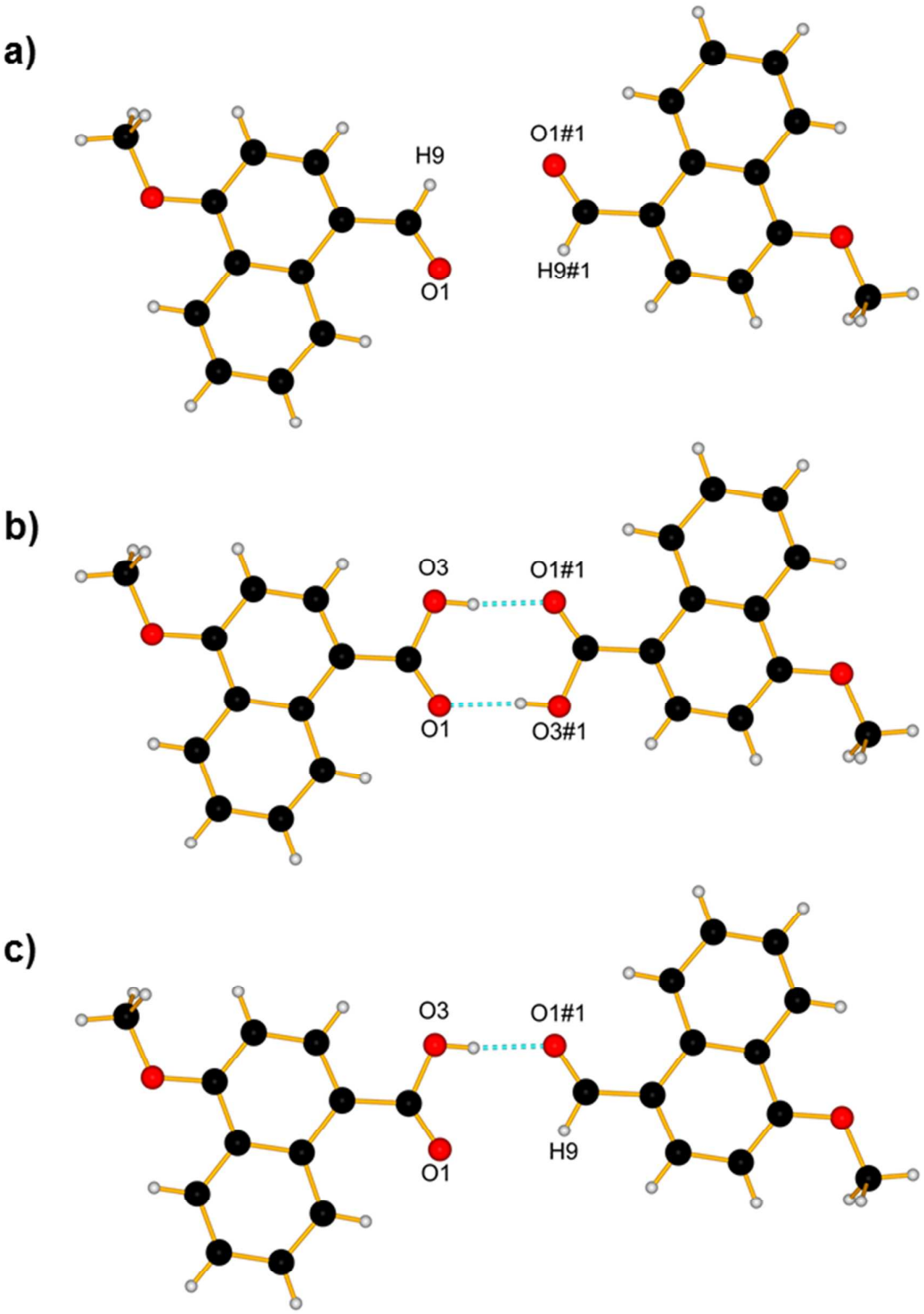

Figure 2. Hydrogen bonding motifs: a) aldehyde-aldehyde; b) acid-acid; c) acid-aldehyde.

Quantum-chemical calculations:

Quantum-chemical calculations were performed by using the Gaussian 09 program suite [19]. If not explicitly described, the M06-2X functional [20] was used with def2-TZVP basis set [21].This fitted hybrid meta-GGA functional with 54% HF exchange is specially developed to describe main-group thermochemistry and the non-covalent interactions, showing very good results in prediction of the position of the tautomeric equilibrium in azo naphthols possessing intramolecular hydrogen bond [22]. All structures were optimized without restrictions, using tight optimization criteria (with only exception in the modeling dimer associates) and ultrafine grid in the computation of two-electron integrals and their derivatives, and the true minima were verified by performing frequency calculations in the corresponding environment. Solvent effects are described by using the Polarizable Continuum Model (the integral equation formalism variant, IEFPCM, as implemented in Gaussian 09) [23].

The deprotonation processes were modeled by gradually changing the O-H distance (r_{O-H}) in steps of 0.1Å and optimizing the rest of the molecule at each step. In the case of **1** additional constraints (fixing the molecule planar and fixing the C-O-H angle as obtained from the equilibrium geometry in the corresponding solvent environment) were used. The rotational barriers, shown in the Supplementary information, were modeled by gradually changing the corresponding dihedral angle in steps of 10^{o} and optimizing the rest of the molecule at each step. The full counterpoise method [24] was applied to correct the basis set superposition error (BSSE) on the dimers.

The absorption spectra of the compounds were predicted using the TD-DFT formalism. TD-DFT calculations were carried out at the same functional and basis set, which is in accordance with conclusions about the effect of the basis set size and the reliability of the spectral predictions [25,26].

Results and discussion

The absorption spectra of **1**-**3** in various solvents are shown in Figure 3. In toluene all compounds show the same spectral shape – a structured band at 320 nm in the case of **1** and **3** and red-shifted absorption at 340 nm for **2**. In acetonitrile and methanol a new band in the region 360-400 nm appears in the case of **1** and **2** only. Its strength depends on the solvent and the compound – it is very low in the case of **1** in acetonitrile and dominating in **2** in methanol. In addition, as will be discussed below, in **1** the intensity of this band rises in methanol and acetonitrile with decreasing concentration.

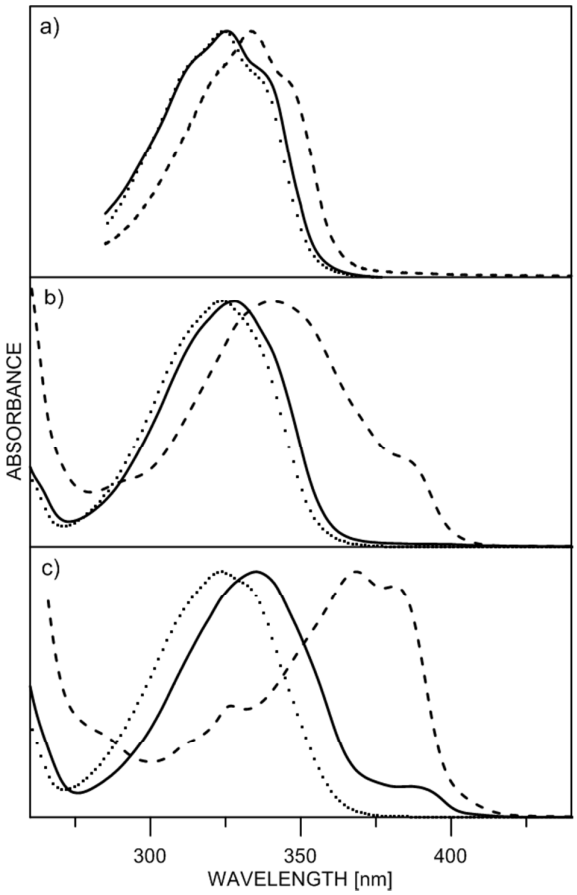

Figure 3. Normalized absorption spectra of **1** (solid line), **2** (dashes) and **3** (dots) in toluene (a), acetonitrile (b) and methanol (c).

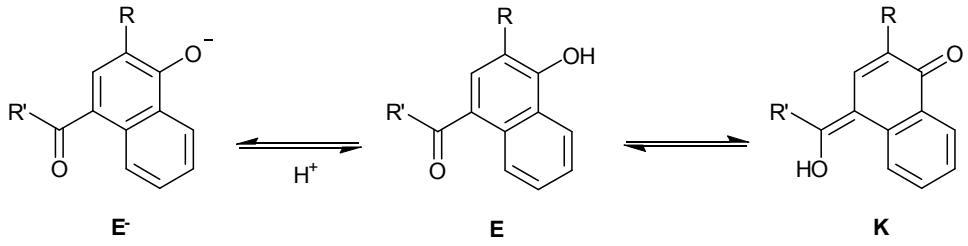

Scheme 2. Deprotonation (left) and tautomerism (right) in **1**, **2** and **4**.

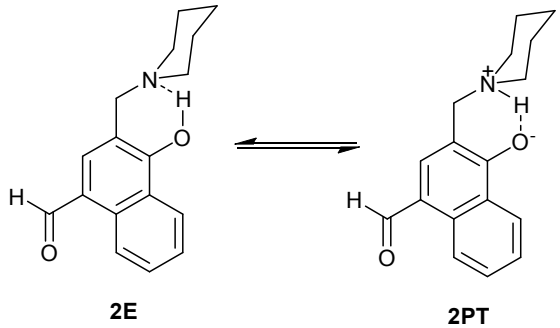

Scheme 3. Intramolecular proton transfer in **2**.

Taking into account that the spectra of **3** (fixed enol) do not change with the solvent, the appearance of this new species for **1** and **2** can be interpreted in the light of two possible processes – tautomerism or deprotonation, as shown in Scheme 2. In addition, a process of internal deprotonation through proton transfer is possible in the case of **2** (Scheme 3) as observed in some azonaphthols [27] and Mannich bases [28,29,30]. According to the results obtained from the quantum-chemical calculations, given in Figure 4, the **E**-tautomer is much more stable and its stabilization is supported by the intramolecular hydrogen bonding involving the piperidine antenna in **2**. Although the keto tautomer is more polar (for instance: 6.7D against 4.3D in **1** in gas phase) the effect of the solvent polarity does not provide conditions for shifting the equilibrium towards latter. In addition to that, the content of the component absorbing at 380 nm is substantially higher in the case of **2**, which seems impossible in the light of the proven enol stabilizing action of the piperidine antenna [7]. Going further – even if the keto form of **2** (**2K**) would be stabilized somehow and exist in methanol and acetonitrile, the addition of acid would further boost this process, as suggested by Figure 4 and results for other, structurally similar tautomeric systems [7,9,11]. Upon addition of acid the absorption spectra of **1** and **2** in methanol or in acetonitrile show no rise, but disappearance of the band at 380 nm and restoration the original band at 320-340 nm (see Figure 5 for **2**). The fact that this happens in both compounds is clear evidence that no tautomerism, but a protonation equilibrium is originally observed in solution. At the same time, there are no spectral changes in the case of **3**, in which the relevant hydrogen atom is replaced by a methyl group, in the same pH interval.

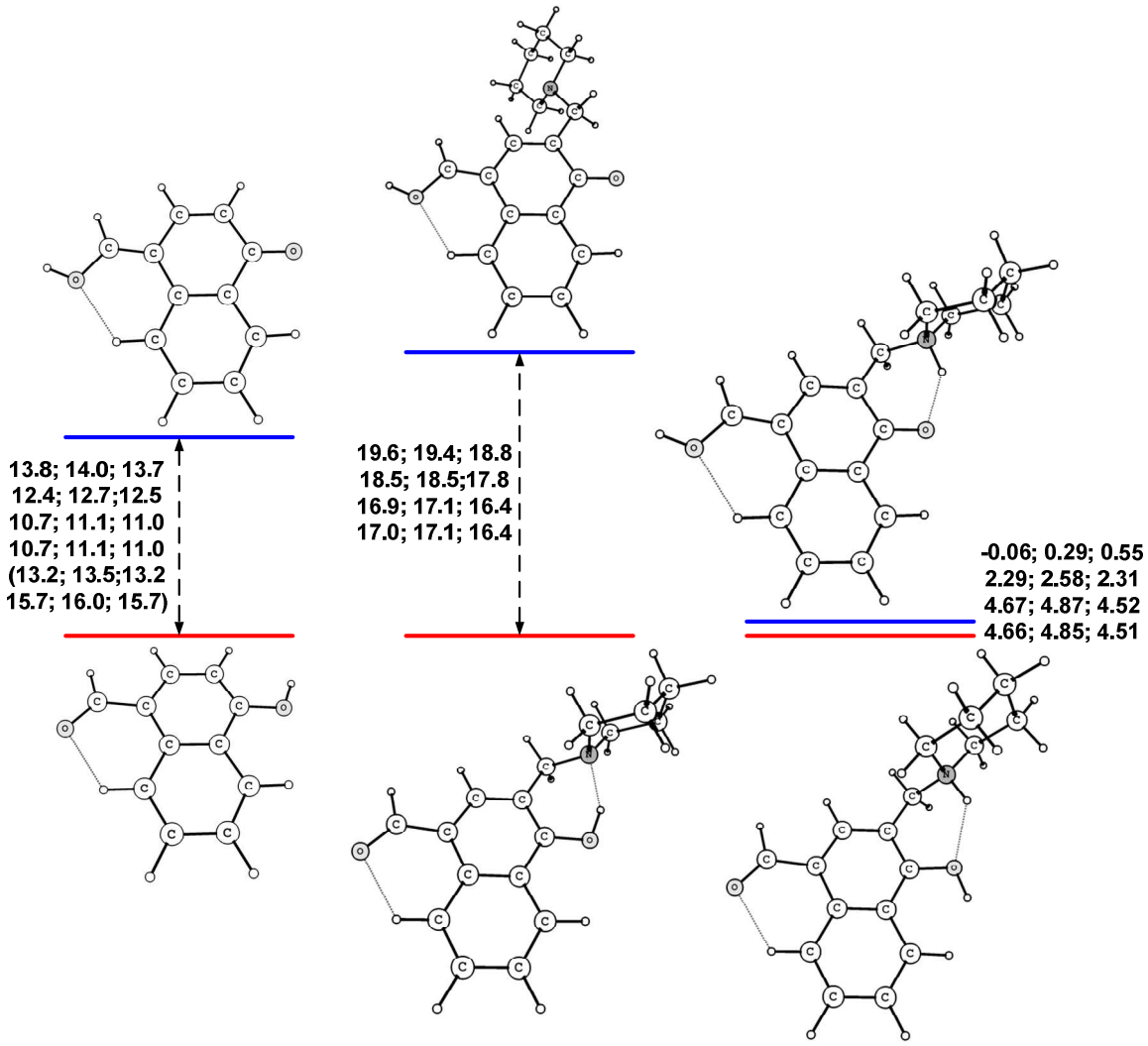

Figure 4. Predicted relative stability (M06-2X/def2-TZVP) of the tautomers of **1**, **2** and **2H**$^+$ in gas phase, toluene, acetonitrile and methanol. Each row shows the relative energy ($\Delta E=E_K-E_E$), ΔE+ZPE and ΔG (298K) values in the corresponding solvent in kcal/mol units. The energy gaps are scaled according to the gas phase results. The values for **1** in gas phase using HF and MP2 are given in parentheses. In the figure the most stable isomers of each tautomer are presented, for details see Part 2 of the Supplementary Information.

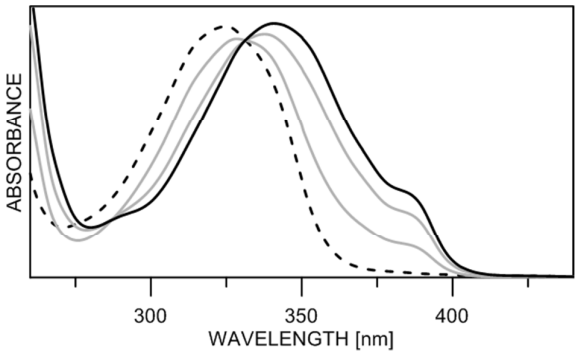

Figure 5. Absorption spectra of **2** in acetonitrile upon addition of H_2SO_4: pH=6.9 (solid black line, 27% deprotonated form), 4.8, 4.0, 3.5 (dashes).

In order to supplement the information already obtained from UV spectra, NMR spectra have been recorded in the same solvents in order to characterize the various species, the **E**$^-$, **E** and **PT**-forms. ^{13}C NMR data are given in Table 1. The ^{13}C spectrum of **2** in toluene is that of the **E**-form, whereas that in CD_3OD is close to that of the deprotonated form. In $CDCl_3$ ^{13}C chemical shifts slightly different from those in toluene-d_8 are obtained (Table 1), whereas in CD_3CN characteristic variations are seen. Addition of base to the sample in CD_3OD as well as low temperature spectra of **2** in $CDCl_3$ have also been recorded, the latter in the temperature interval from 298 K to 213 K (Table 1).

Table 1. Experimentally measured ^{13}C chemical shifts of **2**.

	Toluene-d_8	$CDCl_3$	$CDCl_3$ 213 K	CD_3CN	CD_3OD	CD_3OD + base [a]	CD_3CN + acid [b]
C-1	123.7	122.5	120.1 (2.4)[c] [0.8][d]	122.0	118.4	115.7	125.5
C-2	138.5	138.9	141.0 (-2.1) [0.5]	141.2	145.4	148.1	142.7
C-3	112.9	112.7	111.2 (1.5) [2.0]	113.5	111.5	119.2	114.6
C-4	161.3	162.2	165.2 (-3.0) [-2.9]	165.3	174.3	177.6	160.0

C-5	123.0	122.7	122.7 (0) [-0.1]	123.8	125.3	126.3	123.6
C-6	126.0	125.8	125.4 (0.4) [0.4]	126.6	125.8	124.6	128.1
C-7	129.4	129.3	129.5 (-0.2) [0]	130.1	130.6	129.6	131.5
C-8	125.2	124.5	124.5 (0) [0.1]	125.4	125.8	125.6	125.9
C-4a	125.7	125.2	125.6 (-0.4) [-0.2]	126.4	129.8	131.3	126.0
C-8a	132.4	131.9	131.8 (0.1) [-0.1]	132.9	135.3	135.5	133.8
CHO	190.6	191.6	192.0 (-0.4) [0.2]	192.3	192.1	190.9	193.1
CH2	61.6	61.7	61.4	61.9	60.9	58.3	56.9
C-2´,6'	53.6	53.6	53.1	54.0	53.8	55.1	54.4
C-3´,5'	25.9	25.6	25.0	26.3	25.2	26.7	23.7
C-4'	24.0	23.7	23.0	24.2	23.5	25.5	22.2

[a] Potassium t-butoxide; [b] Trifluoroacetic acid is added; [c] Difference between chemical shift at 298 K and 213 K; [d] Calculated chemical shifts for a lengthening of 0.1 Å; piperidine unit carbons are designated as prime (').

In the ^{1}H spectrum of **2** in CD_3CN with trifluoroacetic acid added, a three-bond coupling between CH_2 and the NH proton of 5.2 Hz is observed showing that slow exchange is taking place, but also giving an indicator to be used to establish the amount of the proton transferred form. In the case of **1** no distinct changes are found in the chemical shift of the aldehyde proton when adding methanol, indicating that the aldehyde group is not involved in tautomerism.

The ^{1}H NMR spectrum of **2** at ambient temperature shows a resonance at ~12.5 ppm. The position is very dependent on moisture in the sample. Upon cooling the resonance moves to 14.5 ppm in $CDCl_3$ (193 K), whereas the signal in CD_2Cl_2 moves from 12.4 ppm (ambient) to 12.8 (243 K), 13.05 (223 K), 14.2 ppm (203 K) and 14.45 ppm (193 K), the resonance becoming gradually broader. In acetonitrile the situation is different. At ambient temperature the resonance is at 12.65 ppm, whereas at 243 K the position is 12.75 ppm, which means virtually no change.

In all cases do the flipping of the piperidine ring stop at low temperature leading to distinct resonances at 3.10 ppm (d, 2H), 2.31 (triplet, 2H), 1.93 ppm (triplet like, 1H), 1.70 (triplet, 2H) and 1.70 (two broad triplet, 3H) and 1.22 ppm (m,1H).

Having established no aggregation of **2** at ambient temperature (no variation of the absorption spectra with the concentration) and in acetonitrile clearly seeing two different UV-Vis bands (Figure 1), an equilibrium has to exist between the **E**- and **PT**-form. This equilibrium is shifted further towards the **PT**-form in methanol-d_4 as judged from the ^{13}C NMR spectrum. One question also raised by Limbach et al. [31] is the change in the XH chemical shift towards higher frequencies upon cooling in freons. Is this just due to a strengthening of the hydrogen bond and an elongation of the XH bond or is this due to the presence of a tautomeric equilibrium. Analyzing the ^{13}C NMR data of Table 1 it is obvious that the chemical shifts of **2** in CD_3CN is in between those in toluene-d_8 (which are very similar to those in $CDCl_3$) and those in methanol-d_4. This together with the changes in the ^{1}H XH chemical shifts and the UV observations, suggests that in toluene, $CDCl_3$ and CD_2Cl_2 the enol-form is dominant (2.5:1) as suggested previously, whereas in CD_3CN a tautomeric equilibrium is at play but the enol form is dominant. In methanol-d_4 the **PT**-form is dominant as seen from a comparison with the ^{13}C data for the anion.

Having established that in methanol the **PT**-form dominated for **2**, the NMR parameters of the **PT**-form are now known (Table 1). The NMR parameters for the **E**-form can be measured in toluene-d_8 (Table 1). The data in $CDCl_3$ and in CD_3CN are seen to fall in between with those of CD_3CN most towards the **2PT**. In $CDCl_3$ the change in ^{13}C chemical shifts upon lowering of the temperature can be analysed in terms of a XH bond length change as the changes are not similar to those caused by a change in the tautomeric equilibria. A good correlation is found between the observed and the calculated changes (Table 1).

The process of deprotonation in **1** and **2** is, as expected, backed by the electron acceptor nature of the CHO group, on one side. The spontaneous deprotonation of 4-nitronaphthalen-1-ol and related compounds, leading to equilibrium between neutral and deprotonated forms in organic solvents, has been reported already in the literature [32]. On the other side, the nitrogen atom from the piperidine unit in **2** is actually an attached base, which makes the intramolecular proton relocation from O to N relatively easy. Such internal deprotonation in Mannich bases is also known [28].

The deprotonation of **1** and **2** in acetonitrile is illustrated in Figure 6. The addition of base leads to a rise of the band at 380 nm till full deprotonation. The corresponding pKa values, determined spectrophotomerically using the methodology described in [17], are as follows: 9.09±0.08 and 8.57±0.07 for **1** in acetonitrile and methanol. These data are in good agreement with the value of 6.36 [32,33] reported for 4-nitronaphthalen-1-ol in ethanol/water mixture, taking into account the difference in the electron acceptor nature of the CHO and NO_2 groups and the different media. Compound **2** is practically fully deprotonated in methanol and has a pKa value of 8.4±0.1 in acetonitrile. As seen, the proton can be lost much easier in the case of **2** and also in methanol, compared to acetonitrile. In Figure 7 the deprotonation of **1** was modeled by changing gradually the O-H distance. Starting from the minimum at 0.962Å in gas phase the removal of the proton needs substantial energy and this energy does not depend of the solvent environment as described by the PCM model. The addition of a solvent molecule, which plays a role of proton acceptor, facilitates the process most substantially in the case of methanol. These results match nicely the absorption spectra of **1** in Figure 3 – no deprotonation band in toluene, a very weak one in acetonitrile and a noticeable one in methanol, confirming the role of the solvent in the process. The absorption spectra suggest that the proton is lost much easier in the case of **2**, which is also supported by the quantum-chemical results shown in Figure 8. In this case the piperidine nitrogen atom participates as an attached base, attracting and accepting the proton. As seen in gas phase and in toluene this intramolecular O-N proton transfer does not occur, but in acetonitrile and in methanol solvent environment a stable deprotonated form is obtained at O-H distance of 1.7Å with relative energy of 1.17 kcal/mol in methanol and 1.13 kcal/mol in acetonitrile. It is worth to notice that the proton transfer does not involve the O-H distance only. As seen from Figure 8, right, the transfer of the proton is accompanied by change in the O-N distance (and also structural changes in the whole molecule) with a minimum value at r_{O-H}=1.3Å, which corresponds to the inflection point in Figure 8 left. At this point the proton is actually transferred from the oxygen to the nitrogen atom.

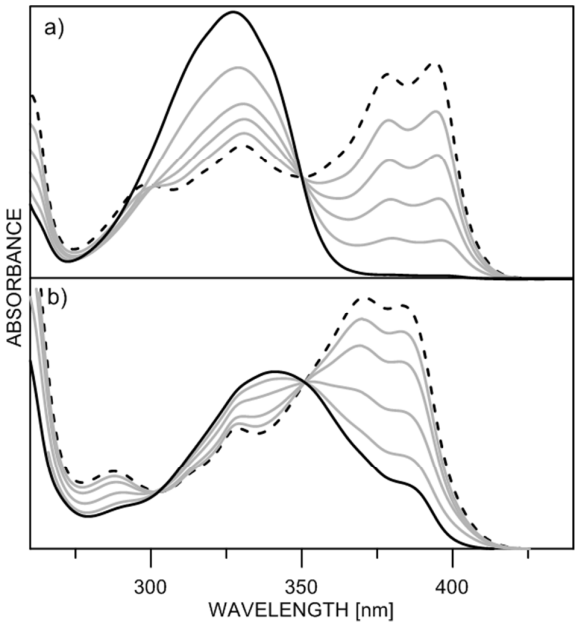

Figure 6. Absorption spectra of **1** (a) and **2** (b) in acetonitrile upon addition of NH_4OH: (a) pH=7.01 (solid black line, 1% deprotonated form), 8.57, 8.93, 9.04, 9.37, 9.68 (dashes, 85% deprotonated form); (b) pH=7.09 (solid black line, 27% deprotonated form), 8.36, 8.51, 9.06, 9.28, 9.59 (dashes, fully deprotonated).

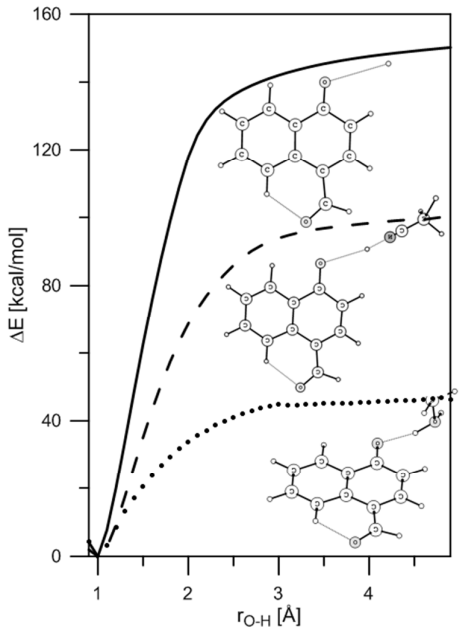

Figure 7. Theoretically predicted potential energy curves for the deprotonation of **1** in gas phase (lines) and interacting with an acetonitrile molecule in an acetonitrile environment (dashes) and a methanol molecule in a methanol environment (points). The deprotonation in toluene, acetonitrile and methanol without participation of a solvent molecule leads to essentially the same results as in the gas phase.

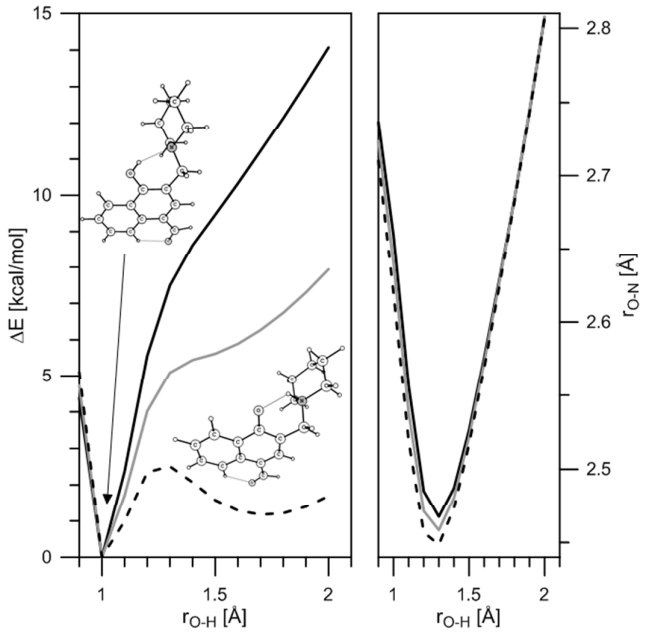

Figure 8. Theoretically predicted potential energy for intramolecular deprotonation of **2** in gas phase (black solid lines), toluene (gray lines), acetonitrile and methanol (dashes) presented as a function of $r_{O\text{-}H}$ (left). Dependence between $r_{O\text{-}H}$ and $r_{O\text{-}N}$ (rigth).

The calculated relative stability of the internally deprotonated (zwitterionic) **2PT** in acetonitrile and in methanol suggests measurable amount of the deprotonated specie in solution, as observed in the absorption spectra, Figure 3, but does not explain the differences between the solvents. Proton donor and acceptor abilities of these two solvents are rather different [34] and the strong proton acceptor/donor capacity of methanol allows formation of complexes with the solute that can additional stabilize one or another form. In addition to the forms shown in Figure 8, compound **2** has one more deprotonated form, which is obtained by rotation of the piperidine ring around the spacer in a way that the piperidine nitrogen atom is at the same side as the CHO group, nearing it (structure **c** in the Figure 9). The situation is clarified in Figure 9 and the possibilities for specific interactions with the methanol are considered in Figure 10. The theoretical calculations show that the intramolecular hydrogen bonded forms **a** and **b** can form complexes with methanol through one of the oxygen atoms. The results suggest that the addition of a methanol molecule leads to stabilization of the deprotonated form **b** through C-O^{-}····HOMe hydrogen bond formation and of the form **a** through CH=O···HOMe interaction. However, the complex of the **b** form is more stable, which reverses the relative energies from Figure 9 and very nicely corresponds to the spectral observation in methanol solution discussed above. The deprotonated **c** isomer offers an additional interaction between the protonated nitrogen atom and the solvent molecule, but all possible complexes are substantially less stable that

the **b** form ones and this isomer cannot exist in solution as also proven by the NMR data (Supplementary information). It is worth to note that the scheme given in Figure 10 is very simplified and does not describe the overall complexity in solution, but it shows the trend to stabilization of the **b** form, explaining its predominance in solution as proven by the spectral data.

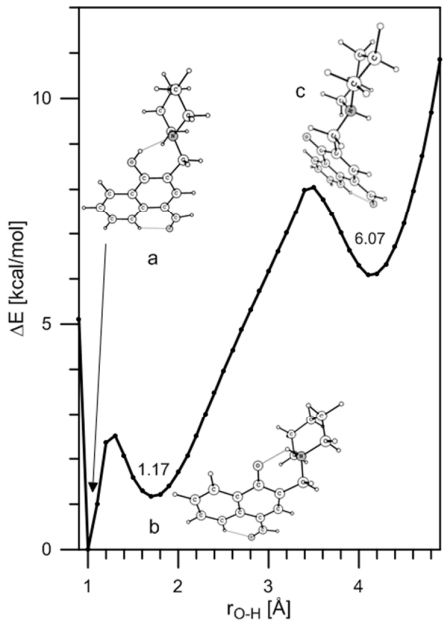

Figure 9. Theoretical description of the rotation of the piperidine ring as a function of the r_{O-H} distance in methanol environment.

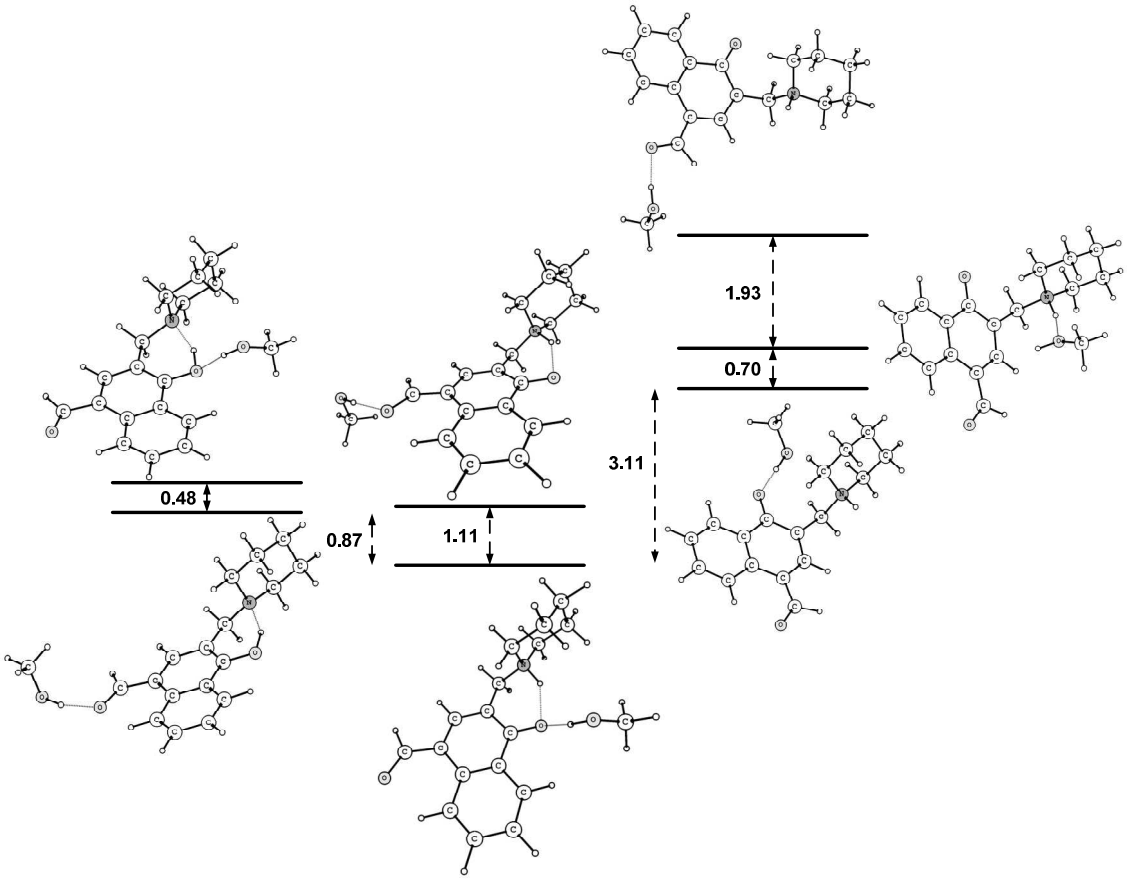

Figure 10. Predicted relative stability (M06-2X/def2-TZVP, in kcal/mol) of the 1:1 complexes of **2** with methanol (from left to right **a**, **b**, **c**, see Figure 9) optimized in methanol environment.

As it was mentioned above, the absorptions spectra of **1** are concentration dependent in both acetonitrile and methanol, as the effect in methanol is more pronounced. The only visual effect of this dependence is the rise of the band of the deprotonated form upon dilution and slight decrease of the intensity at 320-330 nm (Figure 11a). Obviously **1** forms aggregates in solution and their breakup upon dilution facilitates the process of deprotonation. If we assume the simplest case of association in the used concentration region, namely dimerization, the spectral behavior does not allow making clear conclusions about the structure of the dimers. The nearest example is the dimerization of 4-methoxy and 4-ethoxy benzaldehydes, which has been studied in combination between theoretical and experimental (IR and NMR) methods [35]. However, the experimental results do not allow structure of the dimers to be explicitly defined except if crystallographic data are available. In this case, due to the fact that there is no OH group, the theoretical calculations suggest a variety of cyclic dimers involving CHO group and/or the neighbor aromatic C-H atoms, relative stability of which strongly depends on the used level of the theory. The

replacement of the benzene ring with naphthalene in **1** and the availability of free OH group provide four main types, presented in Figure 12, of dimers to be formed. It should be noted that the arrangement of the C=O group towards the neighboring C_8-H in the same molecule reduces substantially the possibility for formation of cyclic dimers via the aromatic CH atoms of the second molecule and such dimers were not found to be stable enough by the theoretical calculations.

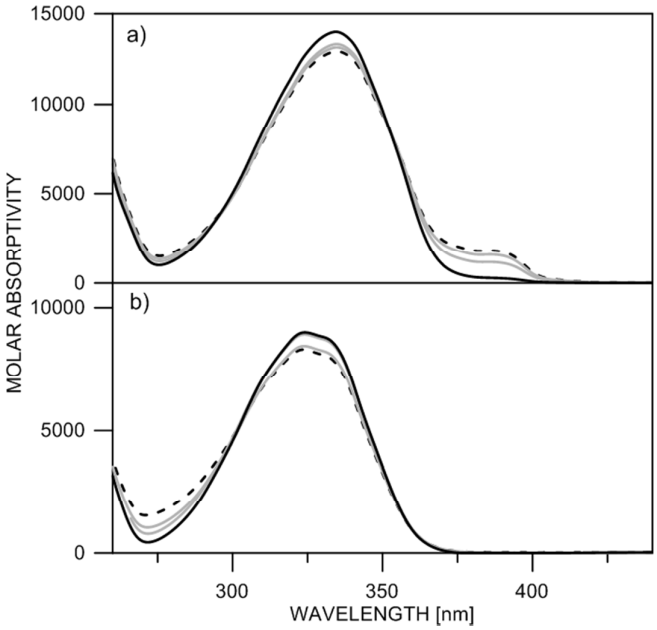

Figure 11. Concentration dependent spectra of **1** (a) and **3** (b) in methanol: solid line – 7.10^{-4} M, dashes – 7.10^{-6} M.

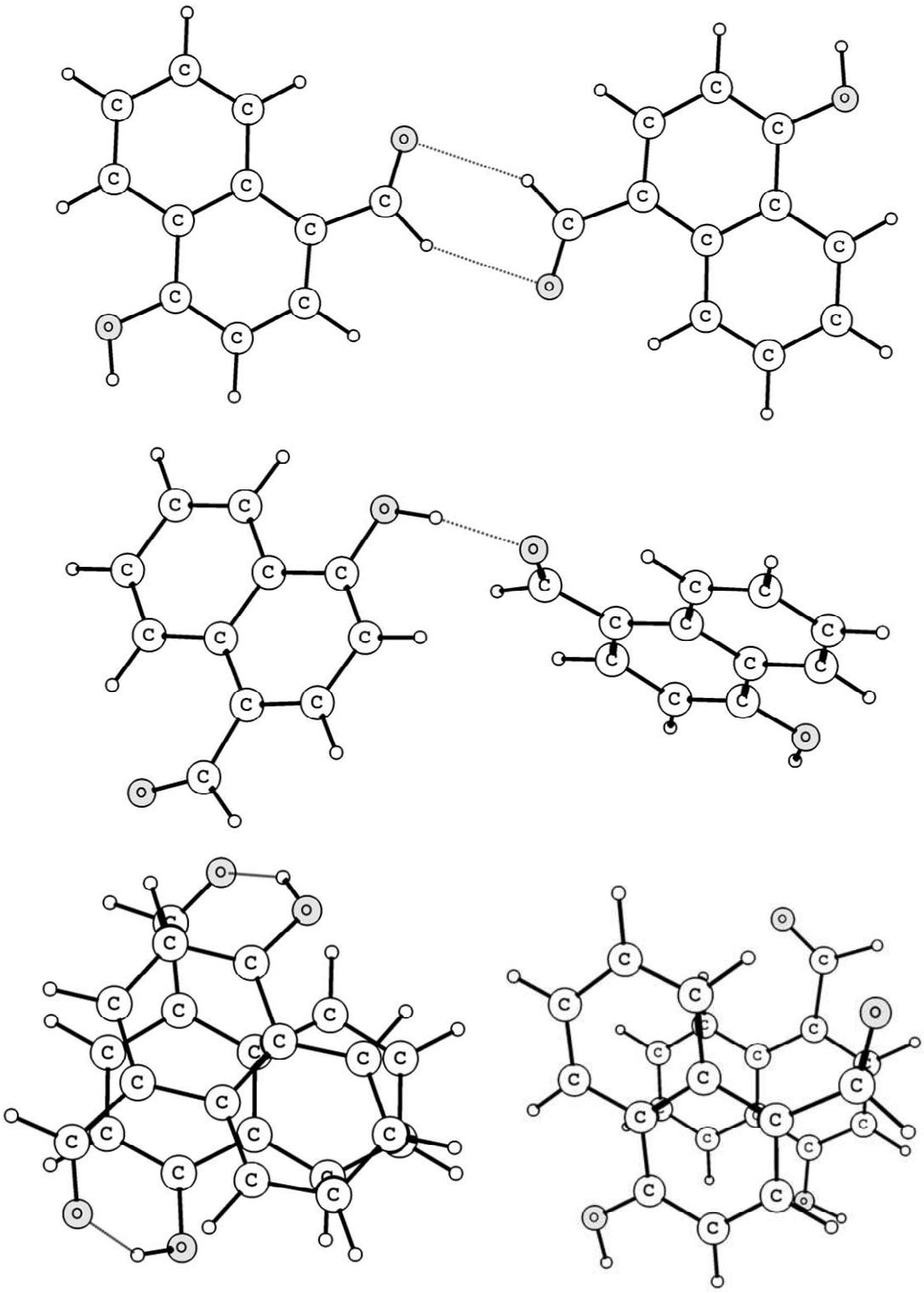

Figure 12. Representative theoretical models of the dimers of **1**: from top to bottom – cyclic, head to tail and sandwich (left: H-bonded; right: π-π stacked).

Each of the dimers, shown in Figure 12, represents the most stable structure from a large number of possible similarities involving isomers of **1** with respect to the orientation of the CHO group (*syn*/*anti*, see Table S3). It is important to note that on the energy scale these three groups are clearly separated. Two of these dimers are formed on the base of hydrogen bonding involving the OH group, which on first glimpse relates them to the deprotonation process. However, the π-π sandwich dimer can also sterically hamper the deprotonation, taking into account the active action of the solvent in this process (Figure 7).

The corresponding stabilization energies, as estimated by the theoretical calculations, are summarized in Table 2, showing that the cyclic dimers are much less stable than the head to tail and sandwich ones. The theoretical calculations predict, taking into account that the M06-2X functional systematically underestimates[†] the band positions [26], a long-wavelength maximum at 360-400 nm, which corresponds to the deprotonated form, the maximum at 320-340 nm is related to the existing strong associates[‡] in solution and the monomer species could be expected to absorb around 290 nm [36].

The limited spectral changes from Figure 11a need additional information to be connected with the theoretical structures from Figure 12. This additional information is found in the spectral behavior of structures **2**-**4**. The spectra of **3** are concentration dependent with appearance of a shoulder at 290-300 nm upon dilution. There is no deprotonation in this case and formation of cyclic or π-π dimers, the absorption maximum of which is red shifted in respect of the isolated monomer (Table 2), is possible. It should be noted here that the steric hindrance of the methyl group probably will reduce substantially the strength of the sandwich dimer comparing with this of **1**. Following the predicted spectral values, the experimentally observed absorbance at 290-300 nm belongs to the monomer and the band at 330 nm can be associated to the dimer. The slight spectral changes suggest a potentially large dimerization constant. The data from Figure 11b were processed as monomer-dimer mixture according to the methodology described in [37], but the slight spectral differences leads only to the rough estimation that the $\log K_D$ value is larger than 6 units. For this reason the spectrum of the pure monomer cannot be extracted. Evidence for a cyclic dimer in **3** is seen from crystallographic data. In solid state, as seen from Figure 2, symmetric dimers exist stabilized by weak C-H···O=C interactions.

The spectra of **2** are concentration independent in the concentration range between 5.10^{-6} M and 1.10^{-3} M. On one side, the dimers through OH groups (head to tail and sandwich) are impossible in this case bearing in mind the steric hindrance of the piperidine unit and the

[†] In order to verify the theoretical results the absorption maxima were predicted by using PBE0 functional in addition. The corresponding results, shown in Table S4, confirm the conclusions about the relative positions of the bands.

[‡] The predicted absorption maxima of the dimers, shown in Table 2, need addition explanation. According to exciton theory [36] the absorption of the sandwich dimer is blue shifted in respect of the monomer. In this particular case (Figure 12, Table 2) the most stable H-bonded sandwich dimer is non-symmetric and the so called J band dominates. The symmetric sandwich dimer, which is less stable by 1.18 kcal/mol (Table S3), has only H-band, which is blue shifted as expected by theory.

involvement of the OH group in strong intramolecular hydrogen bonding. On the other side, cyclic dimers through aldehyde groups cannot be excluded as well as cyclic dimers involving the deprotonated oxygen and protonated nitrogen in **2PT** (Scheme 4). The former cannot be detected through deprotonation peak rise as in **1** since the deprotonation is intramolecular. The latter has been discussed by Limbach et al. [30] and by Sobczyk [38] for a similar compound, 2-(N,N-diethylaminomethyl)3,4,6-trichlorophenol. However, Limbach et al. found dimerization mainly occurred at low temperature and when the solvent as a function of temperature had a high dielectric constant. In order to form a dimer as shown in Scheme 4, the intramolecular hydrogen bond has to be broken and the NH bond rotated 180^{o}. This is illustrated in Figure 9 and is seen to be highly energy demanding and in addition to that entropy non-favored. At ambient temperature both terms cannot be compensated as judged by the Limbach case, but at low temperature the entropy term involved will be less important. Again π-π dimers are possible, but they should be weak bearing in mind steric effect of the CH_2 spacer.

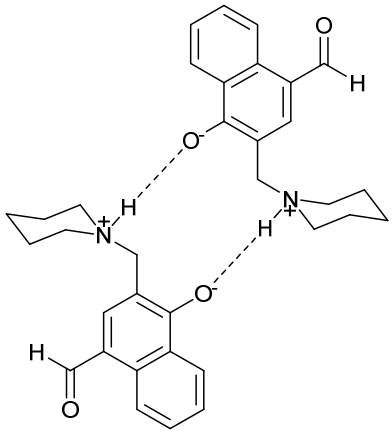

Scheme 4. Sketch of a possible additional type of cyclic dimer of **2PT**.

Compound **4** is a suitable model where cyclic dimers are impossible due to the steric hindrance of the methyl group. The computational and experimental data show that deprotonation occurs in methanol and acetonitrile (Figures S11 and S12), to an extent less than **1**, but the main band is concentration independent. The less monomer (both neutral and deprotonated) is found probably due to the fact that the OH group is less acidic than in **1** because the carbonyl group in **4** is twisted out of the ring plane. The less acidity of the OH group and steric hindrance of the methyl group reduce possibilities for formation of head to tail dimers. At the same time the twisted carbonyl group facilitates interactions in the sandwich dimer, which might explain its stability in this case.

Taking into account the discussion above it is very difficult to find clear explanation of the concentration effect in **1**. Compounds **1**-**4** taking into account the similarity in their structures and spectra exist as aggregates in non-polar solvents. In acetonitrile and especially in methanol the dilution in **1** leads to deprotonation, which indicates that the OH

group is affected by the aggregation process. This excludes cyclic dimers, which are possible in **2** and **3**. The theoretical data from Table 2 indicate that the cyclic dimer is much less stable compared to the head to tail and sandwich ones. The π-π stacking dimer is the only structure that satisfies the observed spectral changes in all studied compounds. Although the OH group is not directly involved in the aggregation, the existence of the dimer hampers the deprotonation process, where the solvent plays active role as shown in Figure 7. This dimer is probably less stable in the case of **2**-**4** for steric reasons, but as the experimental data in the case of **3** show, the dimerization constant even in this case is large enough to fully shift the equilibrium to the dimer in solution. The real situation in solution is much more complicated, because in acetonitrile and especially in methanol additional stabilization/destabilization of the dimers through solvent interaction with the OH and C=O groups can be expected. In this respect the values for the stabilization energies, given in Table 2, must be considered as indicative.

Table 2. Stabilization energies of the dimers of **1** and predicted long-wavelength bands in gas phase.

Structure	ΔE^a [kcal/mol]	Long-wavelength bands	
		λ_{max} [nm]	Oscillator strength
1	0.0	289 296[c] 297[d] 297[e]	0.218 0.318[c] 0.312[d] 0.309[e]
1$^-$	-	330 296 336[c] 295[c] 331[d] 289[d] 331[e] 289[e]	0.233 0.158 0.396[c] 0.207[c] 0.383[d] 0.166[d] 0.379[e] 0.165[e]
2	-	298	0.217
3	-	289	0.246
Cyclic dimer of **1**	3.2 (3.2)[b]	292	0.558
Sandwich π-π dimer of **1**	10.3 (10.2)[b]	301 300	0.046 0.086
Head-to-tail dimer of **1**	10.4 (10.4)[b]	300	0.371
Sandwich dimer of **1**	13.9 (13.9)[b]	332 322	0.026 0.093

[a] Stabilization energy, calculated in respect of the doubled value for **1** ($\Delta E=2.E_{\mathbf{1}}-E_{dimer}$). Positive value indicates stabilization in respect of the monomer; [b] Using BSSE correction; [c] in toluene; [d] in acetonitrile; [e] in methanol.

Conclusions

The experimental results have shown that there is no tautomerism in the case of **1**, but a process of deprotonation, influenced by the solvent and the concentration. The detected aggregation is very strong and influences the deprotonation in acetonitrile and in methanol. The most likely π-π stacking dimer is formed in solution, although in the model compound **3**, a cyclic dimer was proven to exist in the solid state by X-ray measurements. In the case of **2,** intramolecular proton transfer (a kind of internal deprotonation) occurs in acetonitrile leading to an almost full deprotonation in methanol. Although the theoretical calculations explain reasonably well the observed spectral changes, the mechanism of deprotonation in **1** involving the dimer, needs additional investigations.

Compound **1** is not suitable as tautomeric platform for molecular switching, due to the very large energy gap between enol and keto states, which cannot be overcome with the piperidine sidearm as implemented in **2**. Similar behavior has been observed in 4-hydroxyazophenol [7] and in some azonaphthols containing strong electron acceptor substituents [27], where internal deprotonation and formation of zwitterionic structure is observed instead of tautomeric proton transfer.

Acknowledgements

The financial support from Bulgarian Ministry of Education and DAAD (joint research project HTC02/227 Proton Cranes), Swiss National Science Found (SupraChem@Balkans.eu Institutional partnership project) as well as by Bulgarian National Science Found (access to MADARA computer cluster by the project RNF01/0110 and to NMR facilities by projects UNA-17/2005 and DRNF-02-13/2009) is gratefully acknowledged.

References:

1 V. Balzani, A.Credi and M.Venturi, *Molecular Devices and Machines – Concepts and Perspectives for the Nanoworld*, Weinheim*:* Wiley-VCH 2008.

2 J. Steed and J. Atwood, *Supramolecular Chemistry*, Chichester: Wiley 2009**;** J. Atwood and J. Steed, *Encyclopedia of Supramolecular chemistry,* Boca Raton: CRC Press, 2004.

3 P. Franzon, D. Nackashi, C. Amsinck, N. DiSpigna and S. Sonkusale*, Molecular Electronics - Devices and Circuits Technology, IFIP International Federation for Information Processing* 2007, **240**, 1.

4 B. Feringa *(Ed.), Molecular Switches, 2nd edition,* Weinheim: Wiley-VCH 2011.

5 M. Natali and S. Giordani, *Chem. Soc. Rev.* 2012, **41**, 4010; S. van der Molen and P. Liljeroth, *J. Phys, Condensed Matter,* 2010, **22**, 133001; F. Raymo, *Advanced Materials,* 2002, **14**, 401; B. Feringa, R. van Delden, N. Koumura and E. Geertsema, *Chem. Rev.* 2000, **100**, 1789; J.-P. Desvergne and H. Bouas-Laurent, *Chem. Comm*. 1978, 403; D. Leigh, J. Wong, F. Dehez and F. Zerbetto, *Nature* 2003, **424**, 174.

6 P. Liljeroth, J. Repp and G. Meyer, Science, 2007, **317**, 1203; F. Mohn, L. Gross, N. Moll and G. Meyer, *Nature Nanotech*., 2012, **7**, 227.

7 L. Antonov, V. Deneva, S. Simeonov, V. Kurteva, D. Nedeltcheva and J. Wirz, *Angew. Chem. Int. Ed*., 2009, **48**, 7875; L. Antonov, *IAP Conf. Proc.*, 2015, **1642**, 449.

8 H. Y. Lee, X. Song, H. Park, M-H. Baik and D. Lee, J*. Am. Chem. Soc*., 2010, **132**, 12133; A. Farrera, I. Canal, P. Hidalgo-Fernández, L. Pérez-García, O. Huertas and F. Luque, *Chem. Eur. J*., 2008, **14**, 2277; A. Todorov, M. Nieger and J. Helaja, *Chem. Eur. J*., 2012, **18**, 7269.

9 P. J. Taylor, G. van der Zwan and L. Antonov, *Tautomerism: Introduction, History and Recent Developments of Experimental and Theoretical Methods; in Tautomerism: Methods and Theories*, L. Antonov (Ed.), Wiley-VCH, Weinheim, 2013.

10 L. Antonov, V. Kurteva, S. Simeonov, V. Deneva, A. Crochet and K. Fromm, *Tetrahedron,* 2010, **66**, 4292.

11 V. Deneva , Y. Manolova , L. Lubenov , V. Kuteva , F. Kamounah , R. Nikolova and B. Shivachev, *J. Mol. Structr.*, 2013, **1036,** 267.

12 W. Gross, D. Oberkobusch and R. Nemitz, Henkel AG & Co. KGAA, *Agent for dyeing keratin-containing fibers*, US Patent 2010/0064450, Mart 18, 2010.

13 M. L. Rousset, *Bull. Soc. Chim. France* 1897, 300.

14 W. Gu, A. J. Hill, Xi. Wang, C. Gui and R. G. Weiss, *Macromolecules* 2000, **33**, 7801.

15 A. Allen, P. Marquand, R. Burton, K. Villeneuve and W. Tam,*J. Org. Chem.*, 2007, **72**, 7849.

16 L. Antonov and D. Nedeltcheva, *Anal. Lett.*, 1996, **29**, 2055; L. Antonov and D. Nedeltcheva, *Chem. Soc. Rev.*, 2000, **29**, 217.

17 L. Antonov and V. Petrov, *Anal. Bioanal. Chem*., 2002, **374**, 1312.

18 G. M. Sheldrick, *Acta Cryst.,* 2008, **A64**, 112.

19 M. Frisch, G. Trucks, H. Schlegel, G. Scuseria, M. Robb, J. Cheeseman, G. Scalmani, V. Barone, B. Mennucci, G. Petersson, H. Nakatsuji, M. Caricato, X. Li, H. Hratchian, A. Izmaylov, J. Bloino, G. Zheng, J. Sonnenberg, M. Hada, M. Ehara, K. Toyota, R. Fukuda, J. Hasegawa, M. Ishida, T. Nakajima, Y. Honda, O. Kitao, H. Nakai, T. Vreven, J. Montgomery, Jr., J. Peralta, F. Ogliaro, M. Bearpark, J. Heyd, E. Brothers, K. Kudin, V. Staroverov, R. Kobayashi, J. Normand, K. Raghavachari, A. Rendell, J. Burant, S. Iyengar, J. Tomasi, M. Cossi, N. Rega, J. M. Millam, M. Klene, J. Knox, J. Cross, V. Bakken, C. Adamo, J. Jaramillo, R. Gomperts, R. Stratmann, O. Yazyev, A. Austin, R. Cammi, C. Pomelli, J. Ochterski, R. Martin, K. Morokuma, V. Zakrzewski, G. Voth, P. Salvador, J. Dannenberg, S. Dapprich, A. Daniels, O. Farkas, J. Foresman, J. Ortiz, J. Cioslowski, and D. Fox, Gaussian 09, Revision A.02, Gaussian, Inc., Wallingford CT, 2009.

20 Y. Zhao and D. Truhlar, *Theoretical Chemistry Accounts*, 2008, **120**, 215; Y. Zhao and D. Truhlar, *Accounts of Chemical Research,* 2008, **41**, 157.

21 F. Weigend and R. Ahlrichs, *Phys. Chem. Chem. Phys.*, 2005, **7**, 3297.

22 S. Kawauchi and L. Antonov, *J. Phys. Org. Chem.*, 2013, **26**, 643.

23 J. Tomasi, B. Mennucci and R. Cammi, *Chem. Rev*., 2005, **105**, 2999..

24 S. B. Boys and F. Bernardi, *Mol. Phys*., 1970, **19**, 553; S. Simon, M. Duran, J. Dannenberg, *J. Chem. Phys.,* 1996, **105**, 11024.

25 R. Improta, *UV–Visible Absorption and Emission Energies in Condensed Phase by PCM/TD-DFT Methods, in Computational Strategies for Spectroscopy*, V.Barone (Ed.), Wiley-VCH, Weinhein, 2012; D. Jacquemin, B. Mennucci and C. Adamo, *Phys. Chem. Chem. Phys.*, 2011, **13**, 16987.

26 S. Kawauchi, L. Antonov and Y. Okuno, *Bulg. Chem. Comm.,* 2014, **46A,** 228.

27 L. Antonov, V. Deneva, S. Simeonov, V. Kurteva, A. Crochet, K.M. Fromm, B. Shivachev, R. Nikolova, M. Savarese and C. Adamo, *ChemPhysChem,* 2015, **16**, 649.

28 A. Koll and P. Wolschann, *Monatshefte fuer Chemie*, 1999, **130**, 983.

29 E. Haslinger, P. Wolschann, *Monatshefte fuer Chemie,* 1980, **111**, 563.

30 M. Rospenk, L. Sobczyk, P. Schah-Mohammedi, H.-H. Limbach, N. Golubev and S. Melikova, *Magnetic Resonance in Chemistry*, 2001, **39**, S81.

31 P. M. Tolstoy, P. Schah-Mohameddi, S. N. Smirnov, N. S. Golubev, G. S. Denisov and H-H. Limbach, *J. Am. Chem. Soc*., 2004, **126**, 5621.

32 K. Schreiber, M.C.S.S.J. Kennedy Sr., *J. Am. Chem. Soc.*, 1956, **78**, 153; C. Creamer, A. Fisher, B. Mann, J. Packer, R. Richards, J. Vaughan, *J. Org. Chem.*, 1961, **26**, 3148.

33 R. Arnold and J. Sprung, *J. Am. Chem. Soc.*, 1939, **61**, 2475.

34 M. I. Kamlet , J. M. L. Abboud , M.H. Abraham and R.W. Taft, *J. Org. Chem.,* 1983, **48**, 2877; M. Abraham, P. Grellier, J. Abboud, R. Doherty and R. Taft, *Can. J. Chem*., 1988, **66**, 2673.

35 N. Karger, M. da Costa and P. Ribeiro-Claro, *J. Phys. Chem*., 1999, **103A,** 8672; M. Marques,M. da Costa and P. Ribeiro-Claro, *J. Phys. Chem.,* 2001, **105A**, 5292; P. Vaz, M. Nolasco, N. Fonseca , A. Amado, A. da Costa, V. Felix , M. Drew, B. Goodfellow and P. Ribeiro-Claro , *Phys. Chem. Chem. Phys*., 2005, **7**, 3027.

36 M. Kasha, H. Rawls and M. El-Bayomi, *Pure Appl. Chem.,* 1965, **11**, 371.

37 L. Antonov, G. Gergov, V. Petrov, M. Kubista and J. Nygren, *Talanta,* 1999, **49**, 99.

38 L. Sobczyk, *Appl. Magn. Reson.*, 2000, **18**, 47.